Numerical investigation of electric charge measurement by PWP method at solid and liquid interfaces

Valentin Berry, Liren Zheng, Paul Leblanc, Stéphane Holé, Thierry Paillat

Numerical investigation of electric charge measurement by PWP method at solid and liquid interfaces.

V. Berry[1], L. Zheng[2], P. Leblanc[1], S. Holé[2], T. Paillat[1]
[1]Institut Pprime – Université de Poitiers – CNRS – ISAE ENSMA, 11, Boulevard Marie et Pierre Curie, 86073, Poitiers Cedex 9, France
[2]Laboratoire de Physique et d'Etude des Matériaux – Sorbonne Université – ESPCI Paris, PSL Université – CNRS, 10, Rue Vauquelin, 75005, Paris, France

Corresponding author: Valentin BERRY
e-mail address: valentin.berry@univ-poitiers.fr

***Abstract*—**When a liquid contacts a solid, physicochemical reactions form an electrical double layer (EDL) at the interface. Understanding the EDL is crucial to prevent electrical device failures, but few experimental methods can access this charge distribution. Recently, the pressure wave propagation (PWP) method has been explored. This paper presents simulations of current generated by a pressure wave through the EDL using the finite difference time domain (FDTD) method. A parametric study investigates the effects of EDL parameters and stimulus properties on the signal. Simulations with EDL data obtained experimentally for both conductive and dielectric liquids are carried out.

Keywords—Electrical Double Layer, liquid space charge measurements, interface, liquid, numerical, FDTD.

I. INTRODUCTION

The presence of electrical charges in solid and liquid dielectrics can significantly accelerate their premature aging, particularly by strengthening the electric field and causing partial discharges. A thorough study of these phenomena requires precise, non-intrusive, and direct quantification and localization of charges within electrolytes and insulating liquids, as well as at their interfaces with solid surfaces. To date, the measurement of electrical charges in liquids mainly relies on global methods without spatial resolution, such as impedance spectroscopy, cyclic voltammetry, or flow electrification [1–3]. The Kerr effect technique [4] allows the charge distribution to be mapped, but it requires birefringent properties that only a few liquids possess.

Several methods exist to measure the space charge distribution in solids. All of these methods rely on the use of a stimulus that disturbs the electrostatic equilibrium of the charges, inducing an electrical signal that is then analyzed. Among these techniques are the Pulsed Electro-Acoustic (PEA) method, which uses an electro-acoustic wave as a stimulus [4, 5, 6], the Thermal Step Method (TSM), which is based on a thermal front [7, 8, 9], and the Pressure Wave Propagation (PWP) method, which uses a pressure wave [10]. Recently, various works has been conducted to adapt these techniques to the study of charges in liquids and at solid/liquid interfaces [11, 12]. Although this work is still in its very early stages, the results are encouraging but raise some questions regarding the adaptation of these various techniques for dielectric and conductive liquids.

The main objective of this study is to demonstrate the feasibility of obtaining an electrical response (current or potential) (Fig. 1) for a dielectric liquid using the PWP method. It also aims to identify the experimental advantages and limitations for the optimization of sensitivity and resolution in the design of measurement systems. This paper thus proposes a numerical exploration of the current response (I_{PWP}).

This numerical analysis is applied to the study of the electric charge distribution at the solid/liquid interface, particularly within the electric double layer (EDL). The EDL, which will be described in detail later, has the advantage of being a stable and reproducible phenomenon, whose characterization primarily depends on maintaining the chemical purity of the solid and liquid under study. A parametric study is presented, taking into account both the properties of the electric double layer, particularly in terms of charge density and distribution, as well as the shape of the stimulus, namely the pressure wave.

II. THEORETICAL APPROACHES

The Pressure Wave Propagation method (PWP) is a non-destructive technique used to measure the electric charge distribution [13], originally in solids. It involves perturbing the electrostatic equilibrium of electric charges by applying a stimulus, typically by propagating a pressure wave p(x,t) through the medium under study (Fig. 2). Depending on the input impedance of the device, the measurement signal is generated either as a time-varying voltage or current signal.

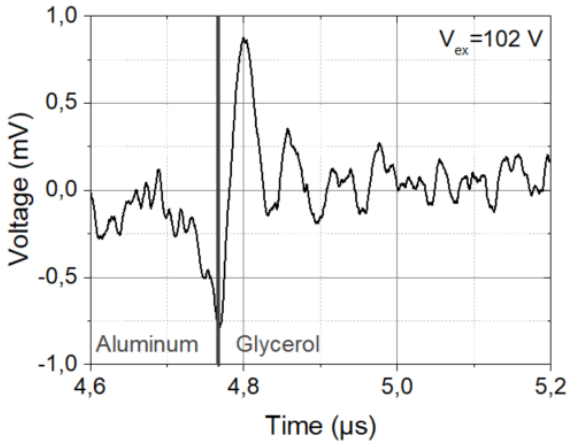

Fig. 1. Experimental measurement of the PWP signal obtained during the propagation of a pressure wave at the aluminum/glycerol interface [12].

The pressure wave is typically generated using a piezoelectric actuator [14] or a laser pulse [15]. The experimental setup consists of two metal electrodes framing a volume of liquid (Fig. 2). As the pressure wave propagates from one electrode to the other through the medium, it induces an electric current $I_{PWP}(t)$ defined by equation (1) [16-17], which correlates with the electric field distribution E(x) and the deformation of the medium S(x,t). A complete demonstration of expression (1) can be found in [17]. This paper focuses specifically on studying the distribution of charges within the electric double layer present at all solid/liquid interfaces.

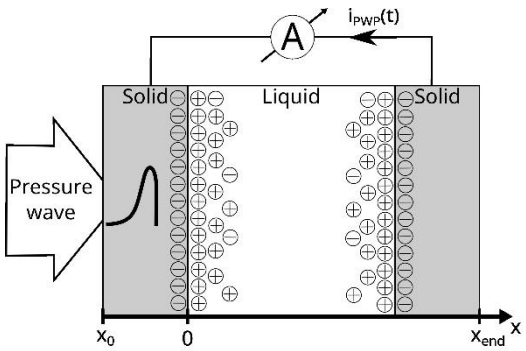

Fig. 2. Schematic diagram of the PWP measurement showing the propagation of the pressure wave from the excitation electrode to the measurement electrode through the liquid.

$$I_{PWP}(t) = -C_0 \int_{x_0}^{x_{end}} \left(1 - \frac{a(x)}{\varepsilon(x)}\right) E(x) \frac{\partial S(x,t)}{\partial t} dx \quad (1)$$

where ε(x) is the permittivity of the medium, a(x) is the electrostrictive coefficient and C_0 is the capacitance between the electrodes that includes the dielectric properties of the liquid between the two electrodes. The medium deformation S(x,t) is directly related to the pressure stimulus p(x,t) by (2):

$$S(x,t) = -\chi(x)p(x,t) \tag{2}$$

where χ(x) is the medium compressibility coefficient.

Furthermore, the electric field is linked to the space charge distribution by the Gauss equation (3).

$$\nabla \cdot \big(\varepsilon(x) \times E(x)\big) = \rho(x) \tag{3}$$

The movement of matter u(x,t) is introduced for expressing strain by (4) and particle velocity V(x,t) by (5).

$$S(x,t) = \frac{\partial u(x,t)}{\partial x} \tag{4}$$

$$V(x,t) = \frac{\partial u(x,t)}{\partial t} \tag{5}$$

The electric field is supposed equal to zero in the depth of the electrodes, and the liquid permittivity and electrostrictive coefficients are assumed constant. Using the previous expressions in (1), $I_{PWP}(t)$ can be defined as:

$$I_{PWP}(t) = -C_0 \left(1 - \frac{a}{\varepsilon}\right) \int_{x_0}^{x_{end}} E(x) \frac{\partial V(x,t)}{\partial x} dx \tag{6}$$

The application of the Clausius-Mossotti relation permits to obtained a calculated value of the electrostricitve coefficient close to the measured value in low-polar materials [18]. In those materials, the value is located in a range from -0.2 to -0.8. For sake of simplicity, *a* is considered equal to -0.5 which providing a new expression of $I_{PWP}(t)$ as (7).

$$I_{PWP}(t) = -C_0 \frac{3}{2} \int_{x_0}^{x_{end}} E(x) \frac{\partial V(x,t)}{\partial x} dx \tag{7}$$

The spatial derivative of the particle velocity in (7) is calculated using the propagation equation (8) solved in the domain by applying the finite difference time domain resolution (FDTD) [19, 20]:

$$\frac{\partial^2 u(x,t)}{\partial t^2} = c^2 \frac{\partial^2 u(x,t)}{\partial x^2} = \frac{C}{d} \frac{\partial^2 u(x,t)}{\partial x^2} \tag{8}$$

where c is the celerity of the medium which is defined according to the compressibility factor C and the density of the medium. Considering equations (4) and (5), two new expressions for the propagation phenomenon are formulated based on the particle velocity V(x,t), and the medium deformation S(x,t):

$$\frac{\partial V(x,t)}{\partial t} = \frac{C}{d} \frac{\partial S(x,t)}{\partial x} \tag{9}$$

$$\frac{\partial S(x,t)}{\partial t} = \frac{\partial V(x,t)}{\partial x} \tag{10}$$

Finally, to induce the propagation of the pressure wave from the solid to the liquid, a source term (11), corresponding to the pressure wave stimulus (p(t)), is incorporated at the x_0 position (Fig. 3) in equation (9).

$$V(x_0,t) = \frac{1}{d_s} \frac{dt}{dx} p(t) \tag{11}$$

where d_s are the density of the solid.

The experimental PWP cell was designed to limit the impact of the wave reflections at the domain limits. This was achieved by adjusting the thickness of different materials in order to sufficiently delay these reflections such that they do not interfere with the initial wave during the measurement window. Therefore, the reflections at the domain limits are not calculated in the simulation. It should be noted that the effects of wave reflection induced at any internal interfaces are obviously taken into account. Thus, for an imposed space charge distribution $\rho(x)$ and pressure stimuli $p(t)$, the $I_{PWP}(t)$ current can be calculated.

A. Space charge distribution: the Electrical Double Layer

When a liquid comes into contact with a solid, physicochemical reactions are triggered, polarizing the solid/liquid interface and inducing two zones of opposite charge polarities known as the electrical double layer (EDL): one within the solid and the other within the liquid. Stern [21] distinguishes within the liquid two sub-layers: the compact layer and the diffuse layer. The compact layer, located closest to the interface, hosts electric charges strongly associated with it. Its thickness is negligible. Beyond the compact layer, the diffuse layer extends, where liquid charges are distributed under the influence of diffusion and migration, among other factors. The volumetric charge density (ρ) is maximal at the interface (ρ_w) and decreases in the direction of the liquid volume according to Boltzmann's law (Fig. 4). ρ_w depends only on the chemical properties of the implicated solid/liquid interface and can be considered as a signature of the interface.

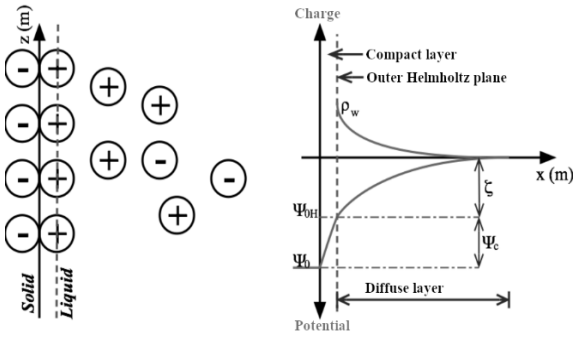

Fig. 3. Organization of the electric charge distribution within the electric double layer (EDL) according to the Stern model.

The diffuse layer thickness is often assimilated to the Debye length δ_0:

$$\delta_0 = \left(\frac{\varepsilon D_0}{\sigma}\right)^{1/2} \tag{12}$$

where σ is the liquid bulk electrical conductivity and D_0 is the mean ionic diffusion coefficient of the liquid charge species. In a first approach, the compact layer may be disregarded. The distribution of the EDL (Fig. 4) in the diffuse layer can be expressed by:

$$\rho(x) = \rho_w e^{\frac{-x}{\delta_0}} \tag{13}$$

The total thickness of the electrical double layer (L_{EDL}) is defined at $3\delta_0$, thickness in which 95% of electrical charges are contained. Whitin a homogeneous conductive solid, the electric field is equal to zero leading to the uniform distribution of electric charges on its surface. The depth of this distribution is likely related to the size of the atomic radius, typically on the order of a tenth of nanometer for a metal. Numerically, to avoid excessive mesh refinement and overly long computation times, the depth of charge distribution within the solid was set to 100 nm. This has negligible effects as long as the pressure pulse extent used in the calculation is much larger than 100 nm. Its value (ρ_s) is imposed in order to ensure the electroneutrality of the solid/liquid interface.

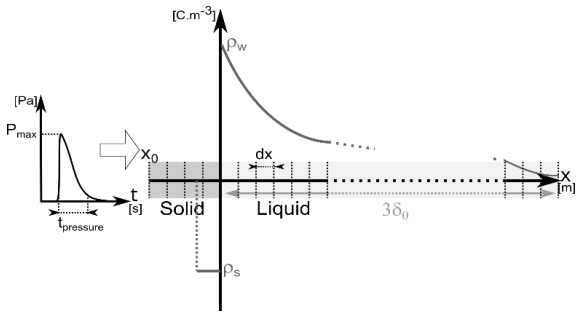

Fig. 4. Description of the simulation domain applied to the numerical study.

Classically, for conductive liquids, ρ_w evolves between 10^2 to 10^4 C.m^{-3} for a δ_0 of a few nanometers while for dielectric liquids, ρ_w evolves between 10^{-4} to 10^{-2} C.m^{-3} for a δ_0 which can reach the millimeter [3].

B. Pressure wave shape

The pressure wave is generated by a piezoelectric actuator. It exhibits asymmetry between its rising and falling phases and is frequently modeled by a double exponential function in the literature [22], Fig. 5. The equation (14), based on the coefficient 4.36, allows to define the maximum amplitude of the pressure wave P_{max} but also its time duration $t_{pressure}$, defined as the time when the pressure is higher than 5% of P_{max} (This time is similar to the 5% response time).

$$p(t) = 4P_{max}\left(e^{\frac{-4{,}36t}{t_{pressure}}} - e^{-2\frac{4{,}36t}{t_{pressure}}}\right) \tag{14}$$

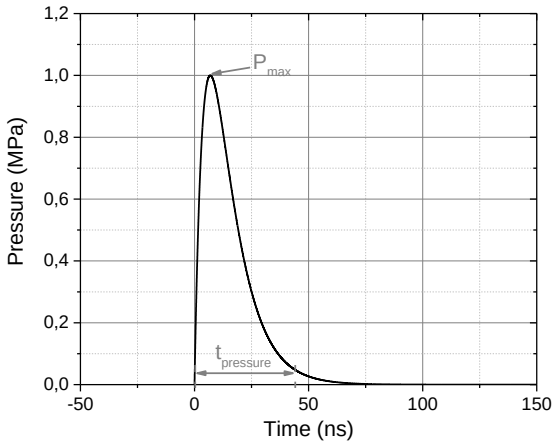

Fig. 5. Temporal profile of the pressure wave imposed on the excitation electrode (P_{max}=1 MPa; $t_{pressure}$=43.56 ns).

III. Calculation Domain and Boundary conditions

The 1-D calculation domain was chosen to simulate only the first solid/liquid interface (Fig. 4), from the excitation electrode to the liquid bulk, corresponding to the interface through which the pressure enters the liquid. This choice is motivated by experimental observations showing that, although the geometry appears symmetrical, the signals measured at the two interfaces are not. Depending on the liquids studied, the attenuation of the pressure wave must be taken into account. The thickness of the solid area is set at L_{solid}=0.25 mm, while the liquid region L_{liquid} extends over 0.5 mm. The radius of the electrode $R_{electrode}$ is 7.5 mm [12], allowing the C_0 value to be calculated by (15) with a relative permittivity ε_r of water equal to 80.

$$C_0 = \frac{\varepsilon_r \varepsilon_0 \pi R_{electrode}^2}{L_{liquid}} \quad (15)$$

The propagation velocity of the pressure wave is modulated by the different media sound velocities. The spatial step dx and temporal step dt are fixed at 50 nm and 5 ps respectively, to comply with CFL conditions (v.dt/dx) equal to 0.642, thus remaining lower than 1.

IV. Typical results

The typical numerical I_{PWP} current over time is illustrated in Fig. 6 for an EDL containing positive charges within the liquid. At t=0 ns, the pressure wave originates from the left side of the solid (x_0). It propagates through the solid before entering the liquid. Initially, the current remains at zero. At 38.75 ns, negative charges within the solid induce a negative current, which increases until reaching a maximum (I_{max}). At the moment when the maximum is reached, the pressure wave crosses the solid/liquid interface. Subsequently, as the pressure wave penetrates the positively charged region of the liquid, it causes a decrease in the absolute value of the negative current. From t=43.85 ns, the current becomes positive and continues to rise until it reaches a positive peak at t=69.33 ns. Thereafter, it gradually diminishes and returns to zero after approximately t=175 ns, coinciding with the pressure wave leaving the charged area of the liquid. This simulated current correlates well with the experimental results (Fig. 1). The time duration (t_{signal}) of the I_{PWP} current is defined from the point when the signal becomes non-zero until it falls below 5% of the amplitude of the second peak. The signal appears as soon as the pressure wave reaches the area in which the charges are situated and disappears when it exits this area. It comes to zero when no more electrical charges are subjected to the action of the pressure wave. The wave propagates through the EDL at speed v_s. Thus, it can be assumed that this signal duration approximately corresponds to the sum of the pressure wave duration and the transit time through the EDL (L_{EDL}/v_s) (16).

$$t_{signal} \approx t_{pressure} + \frac{L_{EDL}}{v_s} \quad (16)$$

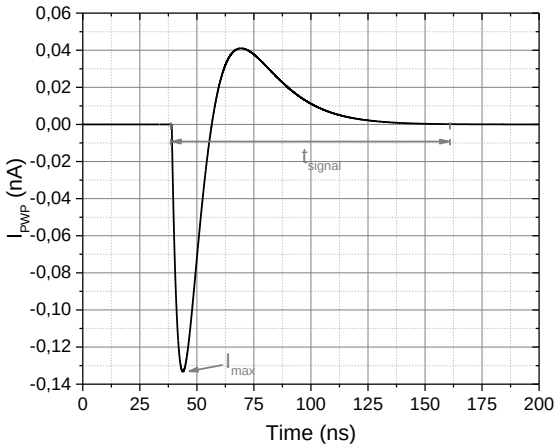

Fig. 6. Typical numerical current response for a positive electric charge distribution in the liquid and a negative one in the solid.

In order to identify the key parameters affecting the amplitude and dynamics of the I_{PWP} current (t_{signal} and I_{max}) a parametric study is carried out. Four parameters are chosen depending on the pressure wave (P_{max}, $t_{pressure}$) and the EDL properties (ρ_w, δ_0).

V. Parametric study

A. *Study of the properties of the pressure wave.*

1) *Impact of pressure wave amplitude (P_{max})*

The analysis ranges from 1 MPa to 50 MPa to scrutinize the influence of the pressure wave amplitude (P_{max}). Throughout the study, the EDL parameters and pressure wave duration remained constant: δ_0=20 µm, ρ_w=10^{-4} C.m^{-3} and $t_{pressure}$=43.56 ns. Figure 7 illustrates the evolution of I_{max} and t_{signal} concerning the pressure wave amplitude. Notably, t_{signal} remains unaffected by variations of P_{max}. Conversely, I_{max} presents a linear correlation with P_{max}, consistent with equations (2) and (14). The amplitude of the electrical response (I_{max}) is proportional to the amplitude of the excitation derivative and thus to P_{max}. Furthermore, since t_{signal} is calculated according to I_{max} and for these simulations the duration of the pressure wave is assumed higher than EDL thickness, t_{signal} only depends on the excitation time.

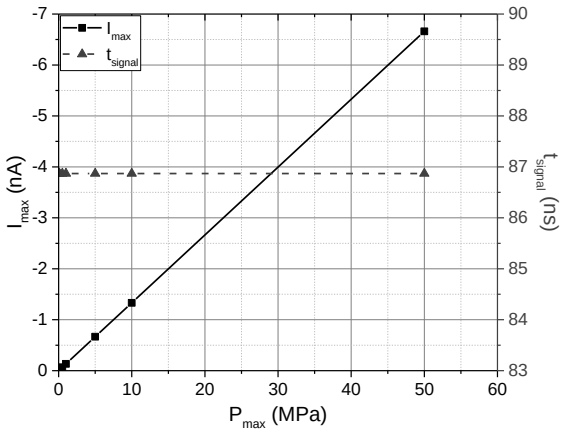

Fig. 7. Evolution of the I_{PWP} properties versus the pressure wave amplitude ($t_{pressure}$=43.56 ns, δ_0=20 µm, ρ_w=10^{-4} C.m^{-3}).

B. Impact of the pressure wave duration ($t_{pressure}$)

The properties of the I_{PWP} current are presented (Fig. 8) as a function of the time duration of the pressure wave normalized by its transit time through the diffuse layer (δ_0/v_s). A noticeable change in the behavior of the two signal properties is observed depending on whether the duration of the pressure wave exceeds or not the transit time through the diffuse layer. Thus, the signal duration is directly proportional to the duration of the pressure wave when it exceeds δ_0/v_s, whereas it becomes independent and converges precisely towards $3\delta_0/v_s=L_{EDL}/v_s$ (the temporal total thickness of EDL) when it is shorter.

Regarding the current, its maximum value decreases as the duration of the pressure wave increases and is relatively insensitive when it is less than δ_0/v_s. The sensitivity and resolution of the measurement are particularly influenced by the relative duration of the pressure wave. It could be particularly well-suited for EDLs exhibiting a thick distribution of electrical charges (deep within the liquid), such as those encountered with dielectric liquids.

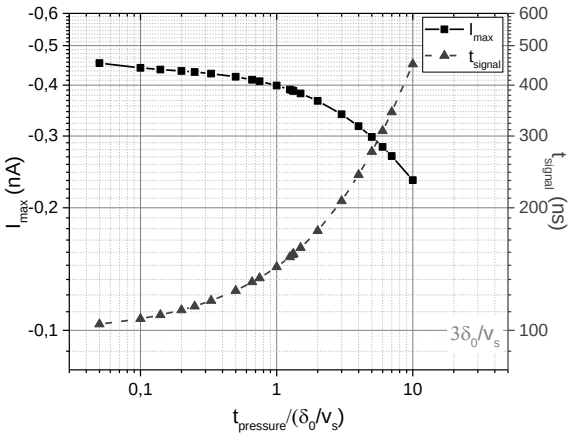

Fig. 8. Evolution of the I_{PWP} properties versus non-dimensional pressure wave duration (P_{max} = 1 MPa, δ_0=20 µm, ρ_w=10^{-4} C.m^{-3}).

C. Study of the properties of the electrical double layer

1) Impact of the space charge density at the wall (ρ_w)

To analyze the influence of ρ_w, the shape of the pressure wave is kept constant ($t_{pressure}$=43.56 ns, P_{max}=1 MPa) and δ_0 is fixed at 20 µm. The studied values of ρ_w are representative of both dielectric and conducting liquids. The higher the space charge density, the higher magnitude of I_{PWP}. The figure 9 illustrates that the maximum current I_{max} increases proportionally as the space charge density increases. Regarding the duration t_{signal}, it remains constant whatever the value of ρ_w. These behaviors are consistent with the equations 1 and 3.

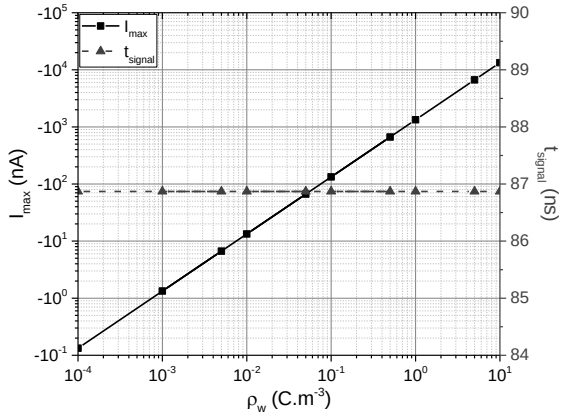

Fig. 9. Evolution of the I_{PWP} properties versus the space charge density at the wall (P_{max} = 1 MPa, $t_{pressure}$=43.56 ns, δ_0=20 µm).

2) Impact of the diffuse layer thickness (δ_0)

The influence of the diffuse layer thickness was investigated by keeping ρ_w at 10^{-4} C.m^{-3} and maintaining the same values for the pressure wave as in the previous section. To obtain sufficient points in the charge distribution in the liquid, the values of δ_0 are chosen as typical values for dielectric liquids, and the extent of the pressure wave always exceeds δ_0. The variation of δ_0 (Fig. 10) directly affects the shape and amplitude of the current. As the pressure wave crosses the electrical double layer, the current amplitude is directly correlated with the number of charges excited in the space simultaneously. The larger the diffuse layer, the higher the maximum current I_{max}. Similarly, the longer the diffuse layer, the longer the duration of the I_{PWP} current.

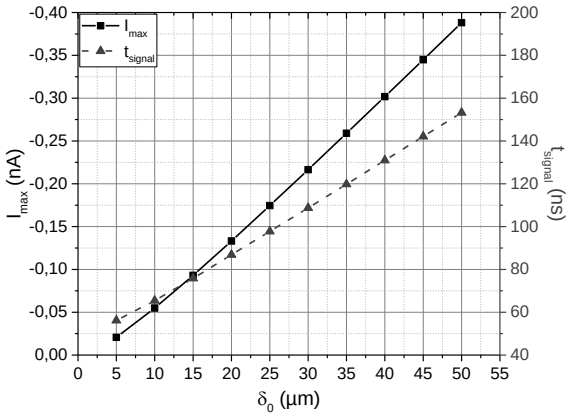

Fig. 10. Evolution of the I_{PWP} properties versus to the Debye length (P_{max} = 1 MPa, $t_{pressure}$=43.56 ns, ρ_w=10^{-4} C.m^{-3}).

VI. APPLICATION TO DIFFERENT SOLID/LIQUID INTERFACES

The electrical double layer is particularly sensitive to the purity of the liquid, especially its electrical conductivity. For example, increasing the liquid's conductivity, by using an additive, reduces the thickness of the diffuse layer (12) while simultaneously increasing the space charge density at the wall. Relying on experimental data extracted from the literature [3, 23], two liquids will be studied: a dielectric liquid (heptane) and a conductive liquid (water). In both cases, the values of ρ_w are extracted from literature and the values of δ_0 are calculated from equation (12).

The pressure wave is set at an amplitude of 1 MPa (P_{max}) for a width of 43.56 ns ($t_{pressure}$) which is always higher than the values of $\delta_0 \times v_s$ (from a factor 2 for the dielectric liquid to a factor of over 1200 for the most conductive liquid). As the depth of the charge distribution is shallower than that studied in the previous section, the temporal and spatial steps are modified maintaining the CFL coefficient constant. (CFL=0.642). The spatial step is fixed to 5 nm and temporal step to 0.5 ps. The charge distribution in the solid is the same as defined in section II-A.

A. Dielectric liquid study

The data used are extracted from flow electrification measurements with heptane containing OLOA 218A as an additive at different concentrations [23]. The properties of the various EDL solutions as well as the simulation results are presented in Table I and Figures 11 and 12. To complete Table I, the celerity of heptane is 1162 m.s^{-1}.

TABLE I. EDL PROPERTIES FOR DIFFERENT HEPTANE CONDUCTIVITIES

Conductivity (S.m^{-1})	**EDL parameters**		
	ρ_w (C.m^{-3})	δ_0 (m)	L_{EDL}/v_s (ns)
$1.00 \cdot 10^{-10}$	$-2.78 \cdot 10^{-3}$	$1.54 \cdot 10^{-5}$	39.76
$1.80 \cdot 10^{-10}$	$-0.50 \cdot 10^{-2}$	$1.14 \cdot 10^{-5}$	29.43
$5.50 \cdot 10^{-10}$	$-2.50 \cdot 10^{-2}$	$6.55 \cdot 10^{-6}$	16.91
$1.00 \cdot 10^{-9}$	$-5.00 \cdot 10^{-2}$	$4.86 \cdot 10^{-6}$	12.55

(D_0=$1.34 \cdot 10^{-9}$ $m^2.s^{-1}$; ε_r=1.99)

In comparison to the previous results, the simulated signals demonstrate a reversal of sign and a higher amplitude (a few nanoamperes), directly linked to the inversion of charge distribution within the EDL and higher values of ρ_w. The rise in heptane conductivity seems to lead to a simultaneous increase of the signal amplitude and a decrease of the signal duration t_{signal}. (Fig. 12). Building upon the findings of the prior parametric study, increasing the value of ρ_w increases I_{max} while decreasing δ_0 decreases I_{max}. According to the results (Fig. 12), the effect of the increase of conductivity seems to be mainly influenced by ρ_w. On the other hand, the decrease of the signal duration is influenced

by the variation of δ_0. Since the duration of the pressure wave and its transit time through the EDL are of the same order of magnitude, reducing L_{EDL} by 30 µm induces a decrease of t_{signal} of the order of 30 ns (Fig. 12).

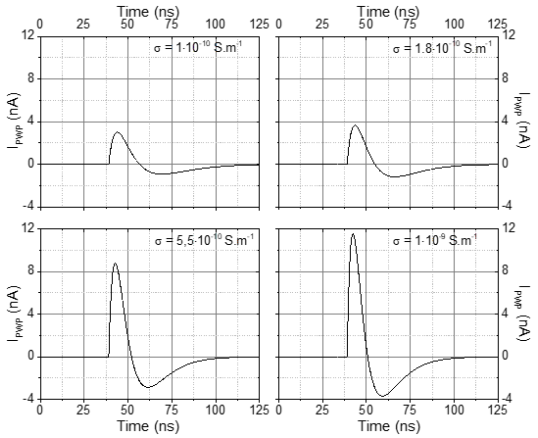

Fig. 11. Evolution of I_{PWP} versus for different conductivities (P_{max}=1 MPa; $t_{pressure}$=43.56 ns).

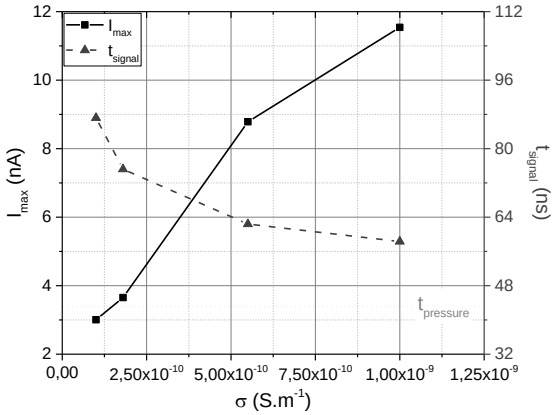

Fig. 12. Evolution of the maximum amplitude and the duration of the calculated signal according to heptane conductivity (P_{max}=1 MPa; $t_{pressure}$=43.56 ns).

B. Conductive liquid study

The data used are extracted from flow electrification measurements [3], where the conductivity of water is modified by the addition of dissolved CO_2. All the data required for the simulations are summarized in Table II. To complete this table, the celerity of water is taken equal to 1500 m.s^{-1}. The figures 13 and 14 respectively depict the temporal evolution of the simulated and mesured PWP current and its analysis based on the two criteria (I_{max} and t_{signal}).

TABLE II. EDL PROPERTIES FOR DIFFERENT WATER CONDUCTIVITIES

Conductivity (S.m^{-1})	**EDL parameters**		
	ρ_w ***(C.m^{-3})***	δ_0 ***(m)***	L_{EDL}/v_s ***(ns)***
$4.00\cdot10^{-4}$	$6.00\cdot10^{3}$	$1.05\cdot10^{-7}$	0.21
$8.00\cdot10^{-4}$	$1.00\cdot10^{4}$	$7.41\cdot10^{-8}$	0.15
$1.20\cdot10^{-3}$	$1.40\cdot10^{4}$	$6.05\cdot10^{-8}$	0.12
$1.60\cdot10^{-3}$	$1.60\cdot10^{4}$	$5.24\cdot10^{-8}$	0.10

(D_0=6.3·10^{-9} m^2.s^{-1}; ε_r=80).

The overall behavior of I_{max} and t_{signal} remains identical to that observed with heptane where the increase of conductivity reduces the signal duration due to the variation of δ_0 and the signal magnitude increases due to the variation of ρ_w. However, in this case, the time duration decreases to a lesser extent, from 45.78 ns to 44.42 ns. This behavior is consistent with the theoretical expectations (12) because L_{EDL}/v_sdecreases according to the function $\sqrt{(1/\sigma)}$. For the highest conductivities, the time duration converges towards $t_{pressure}$. The change in signal polarity is faster than in the previous part. This is caused by the fact that at the interface the variation of space charge density ($|\rho_w-\rho_s|$) is higher for conductive liquids than dielectric liquids (around 1 $C.m^{-3}$ for dielectric liquid and around 20000 $C.m^{-3}$ for conductive liquid).

In order validate these numerical trends, it is possible to compare these results with an experimental campaign using glycerol. The two first peaks of the experimental curves are followed by another one. This peak is obtained because a second little pressure wave is experimentally generated after the first one.

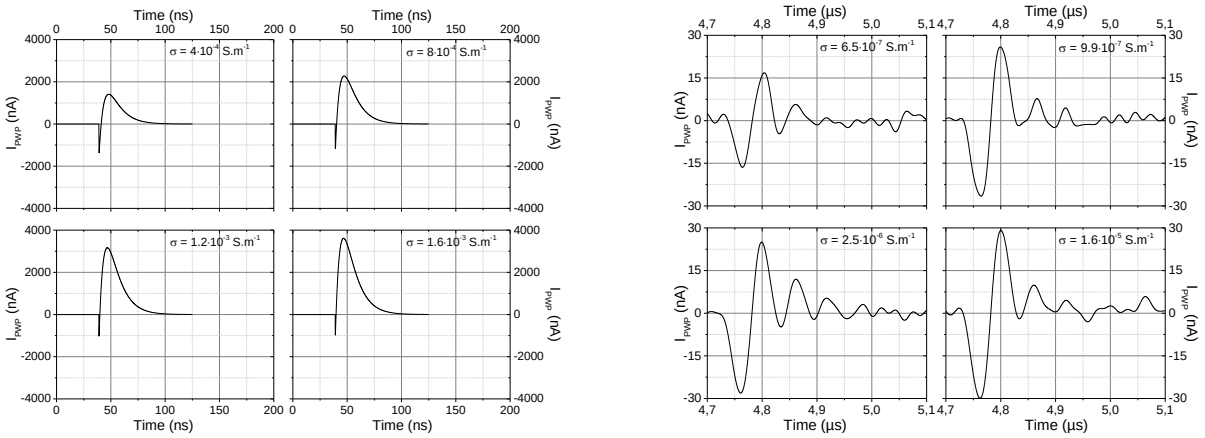

(a) Numerical (b) Experimental

Fig. 13. Evolution of PWP current versus for different water conductivities (P_{max}=1 MPa; $t_{pressure}$=43.56 ns) (a) and evolution of those parameters experimentally obtained versus glycerol conductivity (b).

Regardless of the electrical conductivity, the duration of the signal (t_{signal}) seems to increase while the value of δ_0 theoretically decrease while the liquid conductivity increase (Fig. 14 b). This behavior is not reach experimentally because the conductivity is increase by adding salty water which increase the value of ε too and then of δ_0. Despite that, it shows that t_{signal} is proportional to δ_0 which varies by 17 µm in the conductivity ranges from $6.5\cdot10^{-7}$ to $1.6\cdot10^{-5}$ $S.m^{-1}$. Finally, the behavior of I_{max} remains the same, the higher the electrical conductivity is, the higher I_{max} is.

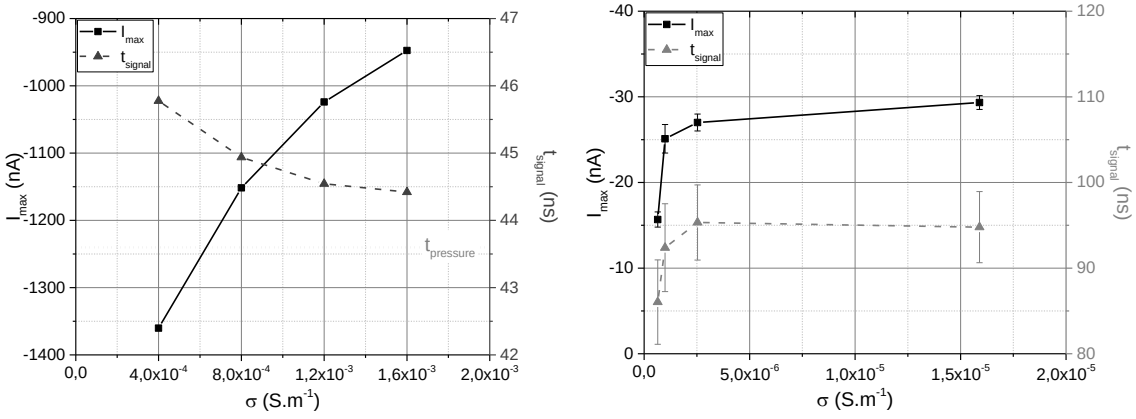

(a) Numerical (b) Experimental

Fig. 14. Evolution of the maximum amplitude and the duration of the calculated signal according to water conductivity (P_{max}=1 MPa; $t_{pressure}$=43.56 ns) (a) and the values experimentally obtained according to glycerol conductivity (b).

VII. CONCLUSIONS

Initial experimental measurements have demonstrated that the PWP technique can effectively probe the electric charge distribution in the EDL for liquids with a conductivity greater than 10^{-7} $S.m^{-1}$. Numerically, it has been demonstrated that the PWP method can measure the electrical response obtained for charge distribution in the EDL in dielectric and conductive liquids. On the one hand, the dielectric liquid gives a low-amplitude electrical response, while the conductive liquid gives a higher-amplitude signal. This information, mainly carried by the value of ρ_w, shows that, for a constant value of C_0 (i.e. constant sample capacitance), the limit in sensitivity of the measurement setup may be reached for measurements in dielectric liquids. To increase the sensitivity of the setup it is possible to reduce the electrode gap, but overlapping the charge distribution at each interface must be avoided. According to the parametric study, the sensitivity can also be modified by increasing the amplitude of the pressure wave. On the other hand, it is shown that the signal duration is directly linked to δ_0 and $t_{pressure}$. With regard to resolution, to obtain a signal dependent on the variation of δ_0, the duration of the pressure wave must be less than the total temporal thickness of the EDL. Experimentally, to measure the electrical response obtained of the PWP method for charge distribution at solid/liquid interfaces with good sensitivity and resolution, the pressure wave must have a high amplitude and as short of a duration as possible.

AKNOWLEDGEMENT

This work is supported by the French Government program “Investissement d’Avenir” (LABEX INTERACTIF, reference ANR-11 LABX-0017-01), “Region Nouvelle Aquitaine” and the European project PLATABAT (2022-23222510).

REFERENCES

[1] Abedian, B., Sonin, A.A., 1982. Theory for electric charging in turbulent pipe flow. J. Fluid Mech. 120, 199–217. https://doi.org/10.1017/S0022112082002730

[2] Walmsley, H.L., 1996. The electrostatic fields and potentials generated by the flow of liquid through plastic pipes. Journal of Electrostatics 38, 249–266. https://doi.org/10.1016/S0304-3886(96)00035-6

[3] Moreau, E., Paillat, T., Touchard, G., 2001. Space charge density in dielectric and conductive liquids flowing through a glass pipe. Journal of Electrostatics 51–52, 448–454. https://doi.org/10.1016/S0304-3886(01)00082-1

[4] Griseri, V., Riffaud, J., Maeno, T., Berquez, L., 2014. Preliminary measurements on dielectric materials by the pulsed electro-acoustic method using a ring electrode, in: Proceedings of 2014 International Symposium on Electrical Insulating Materials. Presented at the 2014 International Symposium on Electrical Insulating Materials (ISEIM), IEEE, Niigata, pp. 112–115. https://doi.org/10.1109/ISEIM.2014.6870733

[5] Wu, K., Zhu, Q., Wang, H., Wang, X., Li, S., 2014. Space charge behavior in the sample with two layers of oil-immersed-paper and oil. IEEE Trans. Dielect. Electr. Insul. 21, 1857–1865. https://doi.org/10.1109/TDEI.2014.004241

[6] Morshuis, P., Jeroense, M., 1997. Space charge measurements on impregnated paper: a review of the PEA method and a discussion of results. IEEE Electr. Insul. Mag. 13, 26–35. https://doi.org/10.1109/57.591529

[7] Cernomorcenco, A., Notingher, P., 2008. Application of the thermal step method to space charge measurements in inhomogeneous solid insulating structures: A theoretical approach. Applied Physics Letters 93, 192903. https://doi.org/10.1063/1.3005425

[8] Sidambarompoule, X., Laurentie, J.-C., Notingher, P., Paillat, T., Leblanc, P., Touchard, G., Toureille, A., Guille, O., 2019. A Non-destructive Thermal Stimulus Method as a Tool for studying the Electrical Double Layer, in: 2019 IEEE 20th International Conference on Dielectric Liquids (ICDL). Presented at the 2019 IEEE 20th International Conference on Dielectric Liquids (ICDL), IEEE, Roma, Italy, pp. 1–4. https://doi.org/10.1109/ICDL.2019.8796837

[9] Notingher, P., Toureille, A., Agnel, S., Castellon, Jé., 2009. Determination of Electric Field and Space Charge in the Insulation of Power Cables With the Thermal Step Method and a New Mathematical Processing. IEEE Trans. on Ind. Applicat. 45, 67–74. https://doi.org/10.1109/TIA.2008.2009612

[10] HoIe, S., 2009. Recent developments in the pressure wave propagation method. IEEE Electr. Insul. Mag. 25, 7–20. https://doi.org/10.1109/mei.2009.4976898

[11] Ndour, A., Holé, S., Leblanc, P., Paillat, T., 2021. Direct observation of electric charges at solid/liquid interfaces with the pressure-wave-propagation method. Journal of Electrostatics 109, 103527. https://doi.org/10.1016/j.elstat.2020.103527

[12] Berry, V., Leblanc, P., Holé, S., Paillat, T., 2024. Space charge measurement at solid/liquid interface by PWP method. Journal of Electrostatics 128, 103894. https://doi.org/10.1016/j.elstat.2024.103894

[13] Lewiner, J., Hole, S., Ditchi, T., 2005. Pressure wave propagation methods: a rich history and a bright future. IEEE Trans. Dielect. Electr. Insul. 12, 114–126. https://doi.org/10.1109/TDEI.2005.1394022

[14] Eisenmenger, W., Haardt, M., 1982. Observation of charge compensated polarization zones in polyvinylindenfluoride (PVDF) films by piezoelectric acoustic step-wave response. Solid State Communications 41, 917–920. https://doi.org/10.1016/0038-1098(82)91235-2

[15] Alquie, C., Dreyfus, G., Lewiner, J., 1981. Stress-Wave Probing of Electric Field Distributions in Dielectrics. Phys. Rev. Lett. 47, 1483–1487. https://doi.org/10.1103/PhysRevLett.47.1483

[16] Zheng, L., Holé, S., 2023. Study of contact conditions at conductor/insulator interfaces used in space charge distribution measurements. Phys. Scr. 98, 025802. https://doi.org/10.1088/1402-4896/acad3f

[17] Holé, S., Ditchi, T., Lewiner, J., 2000. Influence of divergent electric fields on space-charge distribution measurements by elastic methods. Phys. Rev. B 61, 13528–13539. https://doi.org/10.1103/PhysRevB.61.13528

[18] Nakamura, K., Wada, Y., 1971. Piezoelectricity, pyroelectricity, and the electrostriction constant of poly(vinylidene fluoride). J. Polym. Sci. A-2 Polym. Phys. 9, 161–173. https://doi.org/10.1002/pol.1971.160090111

[19] Kane Yee, 1966. Numerical solution of initial boundary value problems involving maxwell's equations in isotropic media. IEEE Trans. Antennas Propagat. 14, 302–307. https://doi.org/10.1109/TAP.1966.1138693

[20] Cole, J.B., Krutar, R.A., Numrich, S.K., Creamer, D.B., 1995. Finite-difference time-domain simulations of wave propagation and scattering as a research and educational tool. Comput. Phys. 9, 235. https://doi.org/10.1063/1.168528

[21] Stern, O., 1924. ZUR THEORIE DER ELEKTROLYTISCHEN DOPPELSCHICHT. Zeitschrift für Elektrochemie und angewandte physikalische Chemie 30, 508–516. https://doi.org/10.1002/bbpc.192400182

[22] Holé, S., Lewiner, J., 1996. Single transducer generation of unipolar pressure waves. Applied Physics Letters 69, 3167–3169. https://doi.org/10.1063/1.116817

[23] Paillat, T., Moreau, E., Touchard, G., 2001. Space charge density at the wall in the case of heptane flowing through an insulating pipe. Journal of Electrostatics 53, 171–182. https://doi.org/10.1016/S0304-3886(01)00139-5